Ground Movements Caused by Diaphragm Wall Installation

L.W. Wong
SMEC Asia Limited, Hong Kong

doi: https://doi.org/10.21467/proceedings.171.24

ABSTRACT

Two-dimensional numerical analysis has been conducted on a case history on ground movements caused by installation of diaphragm walls in soft ground. The trenching was supported with bentonite slurry. Inward ground movements occurs due to the horizontal earth pressures imbalance. The approach of replacing the unit weights of the soil in the trench with that of the bentonite slurry has been adopted. While the slurry supporting the trench has virtually no stiffness, the trench was mainly resisted by the adjacent ground between the primary panels, the concrete wall and gravel infill. This study provides an approximation on the 2-Dimensional analysis on wall trenching. The analysis shows that the surcharge load and the groundwater pressures would affect the ground movements induced by diaphragm wall installation.

Keywords: Slurry trenching, Hardening-Soil Model, Small Strain, Ground Movements

1 INTRODUCTION

Ground movements estimation has been the prime concern of deep excavations. In addition to the main excavation, diaphragm wall installation would also generate some ground movements. Cowland & Thorley (1985), Morton et al. (1980) reported that ground movements induced by diaphragm wall installation could account for 30 % to 50 % of the total settlements induced by the entire excavation activities. The contribution of the ground movements induced by wall installation should, therefore, not be overlooked.

There are studies on the ground movements induced by diaphragm wall installation. Ng et al. (1995) conducted 2-Dimensional (2-D) numerical analysis on 3 wall panels. The analysis results were however not compared with the field observations. Ou and Yang (2011) reported the observed ground movements for a 5-panel test conducted in a Taipei MRT Contract. Based on the observed settlements for the wall construction for the entire station excavation, settlements envelopes were established to evaluate the ground settlements induced by diaphragm wall construction.

In this paper the ground movements induced by diaphragm wall installation for City Hall Station of the Nankang Line of the Taipei Rapid Transit Systems are collected for the study. The Hardening-Soil with Small Strain stiffness (HSS) model have been adopted for the numerical analysis. The stiffness parameters of the soft clay have been established previously by a well-documented excavation case history (Wong, 2023). An innovative approach of replacing the unit weights of the soil in the trench with that of the bentonite slurry has been adopted. Based on the field observations on the case histories of diaphragm wall installation, the virtual stiffnesses of the slurry supporting the trench have been assessed in this study.

2 DIAPHRAGM WALL INSTALLATION

Diaphragm walls are line structures, therefore 2-D analyses will be appropriate to evaluate the effects of diaphragm wall installation to ground movements. However, as depicted in Figure 1, each diaphragm wall is installed panel by panel. Primary panels will be dug first and the cavities made would rely on the pressures of slurry for stability. The middle section of these primary panels will be filled up by reinforced concrete with the remaining two end sections infilled with gravels to provide spaces to join with the secondary panels to form a continuous wall. Therefore, the trench of a diaphragm wall, as the installation proceeds, is supported by the slurry pressures, the reinforced concrete sections, the sections with gravels and the soils yet to be dug. As the sequence of digging of primary panels and secondary panels is to be decided by site managers with considerations given to many constraints, the simulation of the effects of trenching is an extremely difficult

Proceedings DOI: 10.21467/proceedings.171; Series: AIJR Proceedings; ISSN: 2582-3922; ISBN: 978-81-970666-7-2

issue. To simplify the problem to the extent that it becomes manageable, it is proposed to replace the materials in the trench with slurry with a virtual stiffness to be established by back-analyses.

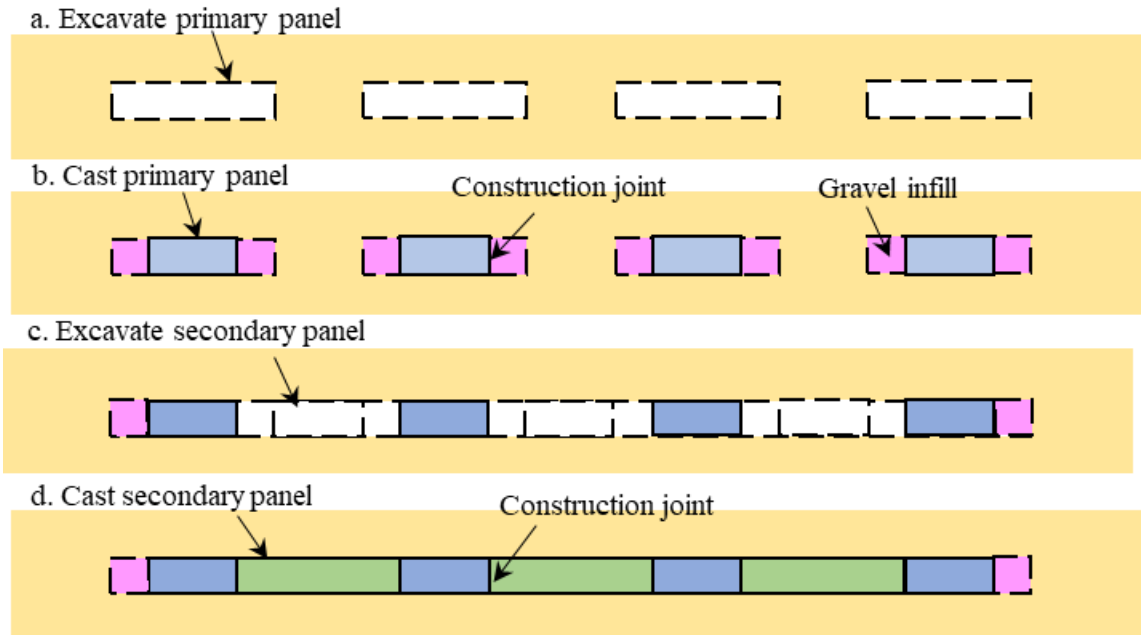

Figure 1: Plan view of the typical sequence for installation of diaphragm wall panels

3 CASE STUDIED

3.1 City Hall Station

City Hall Station of the Nankang Line is located in the K1 Geological Zone at the eastern portion of the Taipei Basin. The excavation case history was presented by Chen et al. (1997). As depicted in Figure 2, the station was 278 m in length and 24 m in width. Inclinometers in ground, SIS2 and SIS3, were deployed on the north and the south sides of the station. The diaphragm wall was 1.2 m in thickness and 44.5 m in depth. The perimeter diaphragm walls for the station and for the ancillary entrances were installed in a 13-month period, starting from November 1992 and with the completion in December 1993.

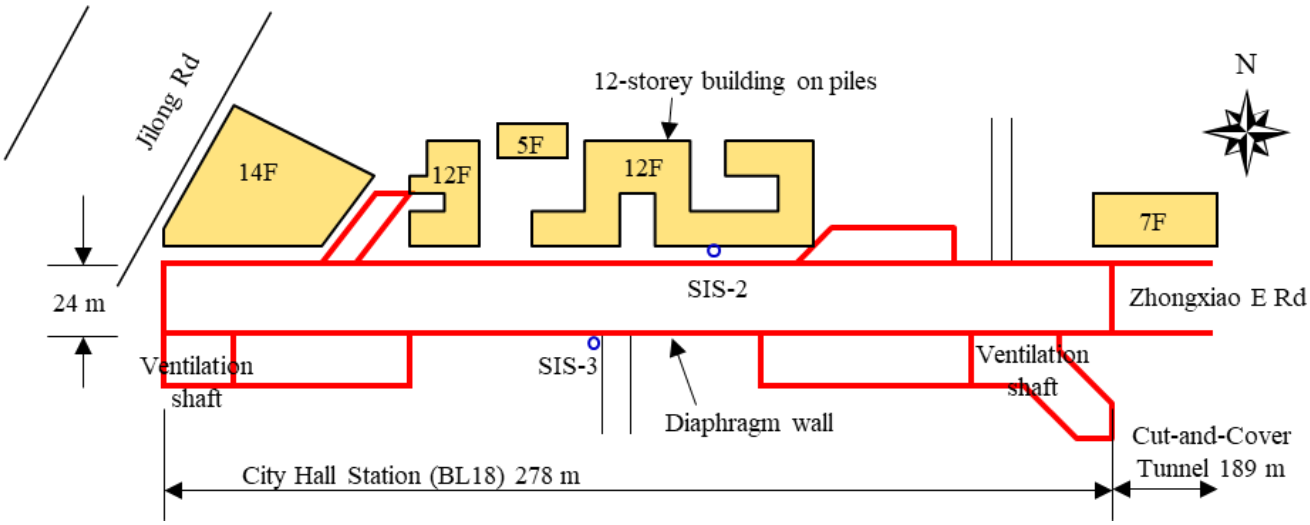

Figure 2: Instrumentation layout of City Hall Station

Proceedings DOI: 10.21467/proceedings.171
ISBN: 978-81-970666-7-2

Series: AIJR Proceedings
ISSN: 2582-3922

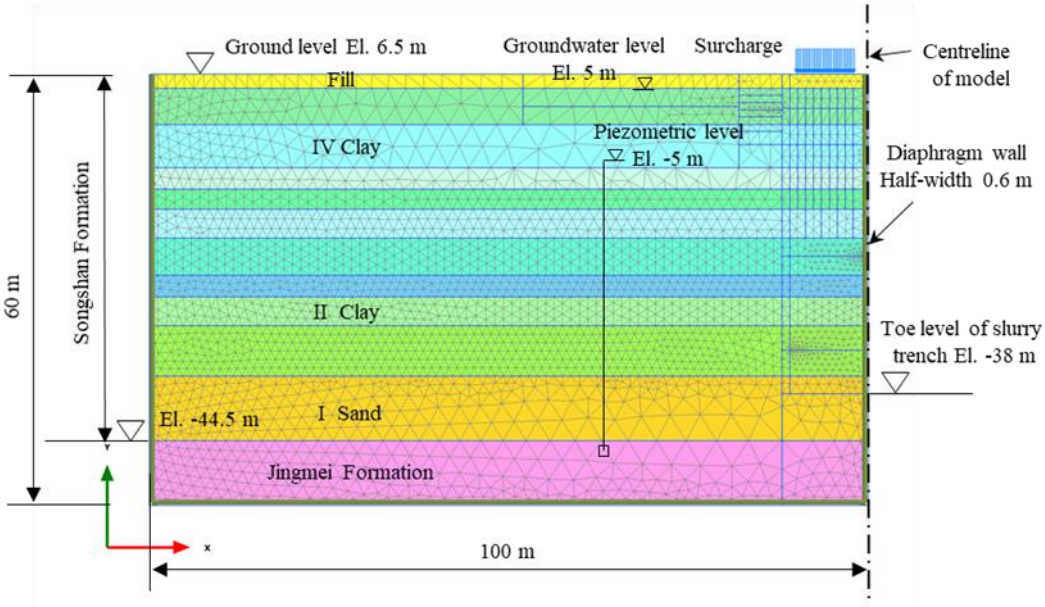

Figure 3: The soil profile and the finite element mesh for the analytical model for City Hall Station

As depicted in the soil profile shown in Figure 3, the total thickness for the clayey Sublayers IV and II of the Songshan Formation is 40 m. The properties of the sublayers in the Songshan Formation have been well discussed in literature (Moh and Ou 1979; MAA 1987; Moh et al. 1989). Underlying the Songshan Formation is a water-rich gravelly (GM) Jingmei Formation, which is a competent formation with very high stiffness.

3.2 Observed ground movements due to wall installation

Monitoring on the inclinometers SIS2 and SIS3 commenced prior to the diaphragm wall installation in November 1992. Figure 4 presents the horizontal ground movements observed in the inclinometers SIS2 and SIS3, which were installed at 2 m behind the diaphragm walls on the north and the south sides of the station respectively. The observation shows that the horizontal ground movements, the δ_h values, gradually developed during the wall installation period. Installation of the first wall panel induced the maximum δ_h values of 17.1 mm and 5.8 mm at inclinometers SIS2 and SIS3 respectively. In the completion stage of wall installation at the end of 1993, installation the full length of diaphragm wall induced the maximum δ_h values of 23.9 mm and 35.6 mm at SIS2 and at SIS3 respectively.

Inclinometer SIS3 is located on the south side of the station, which was an open space utilized as the working area for constructing the southern diaphragm wall of City Hall station. The occurrence of larger δ_h values at SIS3 could be due to surcharge loads imposed from the construction plants.

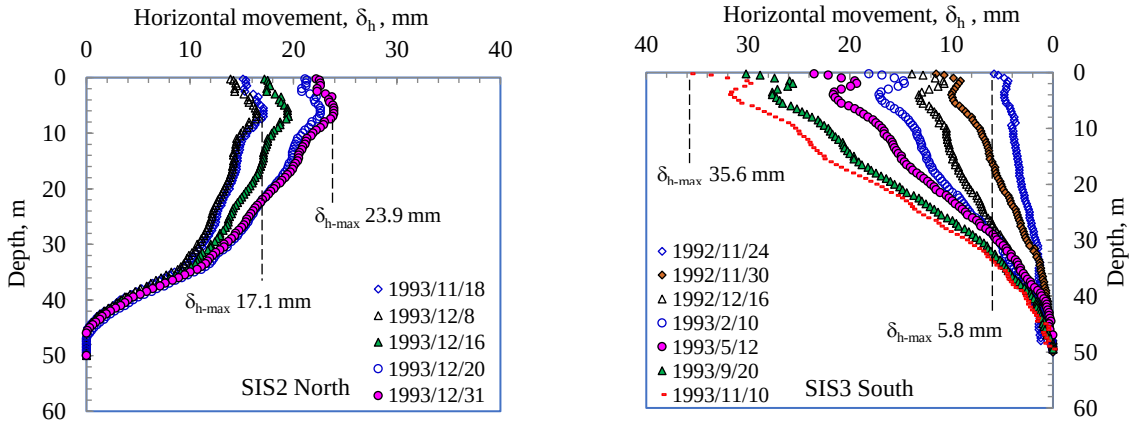

Figure 4: Observed horizontal ground movements on the north and the south sides of City Hall Station

Figure 4 shows the gradual development of the lateral ground movements. After installing the first wall panel in November 1992, the maximum δ_h value of 5.8 mm occurred at SIS3. Installation for the adjacent 24 panels, 12 numbers on the west and 12 on the east sides of the first panel, took 6 months. The maximum δ_h value at SIS3 increased to 23.5 mm in May 1993. Probably due to consolidation, the ground movements continued in the following 6 months with the maximum δ_h value reached 35.6 mm in November 1993.

3.3 Undrained shearing strengths for clay sublayers

An advanced study was conducted by Geotechnical Engineering Specialty Consultant engaged by the Department of Rapid Transit Systems of Taipei City Government in the very early stage of the metro construction. This Designated Task studied the characteristics of the soils in the Taipei Basin to provide the basic information required for the design and construction of metro facilities (Chin et al. 1994 and 2007; Chin & Liu 1997; Hu et al. 1996). This was a research project so it was carried out under stringent supervision. Soil samples of high quality were obtained and tested with great care. The test results are therefore more reliable than those normally obtained. Figure 5 presents the results of the CK_0UC tests conducted on the specimens recovered from borehole R-1 that Chin et al. (1994) reported. Borehole R-1 was located at approximately 50 m to the south of City Hall Station.

Kung et al. (2009) and Ou et al. (2000) also presented the results of undrained shear strength, s_u, for the K1 Geological Zone in the Taipei Basin. The s_u values were determined from consolidated triaxial undrained compression and extension tests conducted on specimens recovered from the clayey Sublayer IV. The specimens were saturated and K_0-consolidated to the in-situ effective stress states. The undrained shear strengths to the vertical effective stresses, the s_u/σ'_v ratio, for the compression tests is 0.29. For the extension tests, the s_u/σ'_v ratio is 0.21. The variation in undrained shear strengths for the compression tests that Ou et al. (2000) and Kung et al. (2009) also reported are presented in Figure 5 for comparison. Compared with the CK_0UC tests reported by Chin et al. (1994), the s_u values obtained by Ou et al. (2000) and by Kung et al. (2009) are somewhat lower. The lower s_u values would likely be attributable to sampling disturbance. Although the specimens were consolidated to the in-situ horizontal stress, such process could not fully compensate the effect due to sample disturbance.

In this study, as depicted in Figure 5, the Author has proposed that the undrained shear strengths of the sublayers IV and II clayey soils of the Songshan Formation in the K1 Geological Zone be expressed by the empirical equation:

$$s_u = 60 + 4.8\ (D - 15) \text{ in kPa} \qquad (1)$$

where D is the depth in metre and s_u is the undrained shear strength in kPa. Moh et al. (1989) reported that the sublayer IV clay of the Songshan Formation have the over-consolidation ratios (OCR) ranging from 4 to 1.25 at the depths between 3 m and 15 m. Oedometer tests conducted by Kung et al. (2009) confirmed that OCR profile. The Author has proposed the s_u value ranging from 50 kPa to 60 kPa at the depths within 15 m.

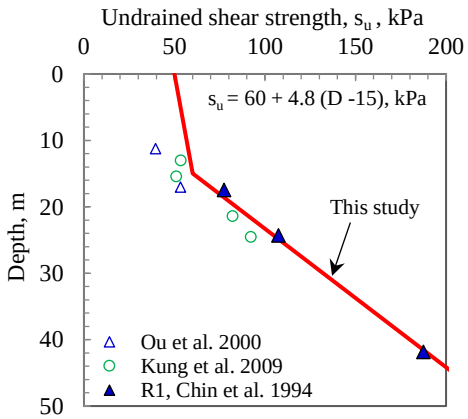

Figure 5: Undrained shear strengths of clays obtained by CK_0UC triaxial tests

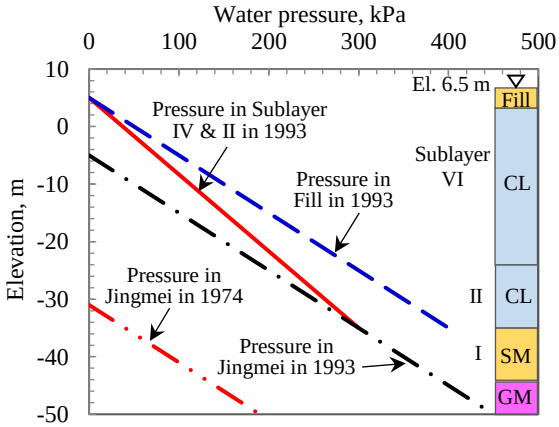

Figure 6: Groundwater pressures distribution in the soil strata at City Hall Station

Proceedings DOI: 10.21467/proceedings.171
ISBN: 978-81-970666-7-2

Series: AIJR Proceedings
ISSN: 2582-3922

3.4 Groundwater conditions

The piezometric level in the Jingmei Formation was lowered to a level near the bottom of the Songshan Formation in the 1970s due to excessive extraction of groundwater to supply water to the city, leading to significant reductions in water pressures in the Songshan Formation and substantial ground settlements as a result. The piezometric level in the Jingmei Formation did not recover till 1974 although pumping had been banned since 1968. The subsoils in the Songshan Formation in the Taipei Basin are thus substantially over-consolidated as the groundwater table rose. This is particularly true for the clayey Sublayer II because the underlying sandy Sublayer I is so permeable that the piezometric level in Sublayer I essentially dropped by the same magnitudes as those in the Jingmei Formation.

Based on monitoring records at the deep well at Sun Yet Sin Memorial Hall, located at 0.5 km east of City Hall Station, Hwang and Moh (2022) reported that the piezometric level in the Jingmei Formation in the eastern portion of the Taipei Basin was around El. -5 m in 1993. In the central portion of the Taipei Basin, the piezometric level in Jingmei Formation recovered to El. 0 m in 2017. The distributions of the water pressures outside the diaphragm wall at City Hall Station in 1993 are presented in Figure 6. For sublayer I and the Jingmei Formation, the piezometric level of El. -5 m in 1993 is adopted. The water pressures for sublayers II to IV are interpolated between the fill layer and sublayer I.

4 NUMERICAL SIMULATION

4.1 Finite element mesh

The section for the 2-D numerical analysis is depicted in Figure 3. The half-width of the excavation trench is 0.6 m. Because of symmetry in geometry, only half of the section is analyzed. The slurry supported trench is assumed to reach a depth of 44.5 m in the analysis. The lateral extent of the finite element model reaches a distance of 100 m from the central axis of the excavation trench. The ground model is 60 m in depth and the diaphragm wall is located along the axis of the trench.

The Jingmei Formation is a competent formation with very high stiffness and is frequently assumed to be the base of the numerical models. However, the base of the finite element model in this study is placed at a depth of 60 m to include a 9 m layer of the Jingmei Formation to ensure that the contribution of this formation to ground movements is accounted for.

4.2 Nonlinearity of soil behavior - Hardening-soil with small-strain stiffness model

The PLAXIS-2D finite element software developed by PLAXIS BV (2013) has become a very popular tool in geotechnical analysis and design. The Hardening-Soil with Small-strain stiffness (HSS) constitutive soil model is an extension of the Hardening-Soil model (Benz 2006, Schanz & Vermeer 1998; Schanz et al. 1999) introduced in the PLAXIS program and is adopted herein to simulate the non-linear stress-strain relationship of soils under loading and unloading conditions. In the HSS model, the parameters adopted to define the hyperbolic stress-strain relationship are as follows:

- E^{ref}_{50} is the reference secant stiffness from standard triaxial drained test,
- E^{ref}_{oed} is the reference tangent stiffness for oedometer primary loading,
- E^{ref}_{ur} is the reference unloading-reloading stiffness from standard triaxial drained test,
- m is the exponential factor for stress-level dependency of stiffness,
- R_f is the failure ratio, $R_f = q_f / q_a$,
- q_a is the asymptotic value of the shear strength and q_f is the failure strength,
- G^{ref}_0 is the reference shear modulus at the level of very small strains,
- $\gamma_{0.7}$ is the reference shearing strain to define the behavior of degradation of moduli when G^{ref}_0 is reduced to 0.7 G^{ref}_0.

In this study, the stiffness values of soils are related to the undrained shear strengths for clays and the N values for sands as expressed in the empirical Equations 2 to 6:

$E^{ref}_{50} = 150\ s_u$ (for clayey soils) (2)

$E^{ref}_{50} = 2\ N$ (in MPa for sandy soils) (3)

$E^{ref}_{oed} = E^{ref}_{50}$ (4)

$E^{ref}_{ur} = 5\ E^{ref}_{50}$ (5)

$G^{ref}_{0} = E^{ref}_{ur}$ (6)

in which s_u is the undrained shear strengths of clayey soils (CL) and N is the blow-counts obtained in standard penetration tests for sandy soils (SM). The parameters adopted in this study are summarized in Table 1. The effective shear strength parameters, i.e., the c' and the ϕ' values, for the silty sand strata, are determined from laboratory tests conducted on specimens trimmed from thin-wall tube samples. For the clayey layers, $c' = s_u$ and $\phi' = 0^o$ are assumed in the analyses. The dilation angle, ψ', of 2^o, 0^o, and 3^o are adopted for the sandy, the clayey and the gravelly soils (GM) respectively. The R_f equals 0.9 is adopted. The unload-reload Poisson's ratio, υ_{ur}, of 0.2 is used as suggested by Benz (2006) and Schanz et al. (1999).

The set of the stiffness parameters in Equations 2 to 6 has been obtained from the small-strain triaxial tests and bender element tests. Wong (2023) verified that set of parameters by a well-documented excavation case history in the K1 Geological Zone of the Taipei Basin.

The HSS soil model is an effective stress model and adopting the $\phi' = 0^o$ for the clayey soils loses its compression hardening function and stress-dependent stiffness. However, parametric studies using both the effective and the total stress models show that the computed wall deflections and settlements are essentially the same. The total stress model for clay is thus adopted in this study.

Table 1: Soil parameters for the HSS model adopted in the PLAXIS analyses – City Hall Station

Mid depth m	Soil type	Unit weight γ' kN/m^3	N value	Undrained shear strength s_u, kPa	Effective cohesion c' kPa	Effective friction angle ϕ', deg	Dilation angle ψ' deg	Reference stiffness, MPa		Initial shear moduli G^{ref}_0, MPa
								Secant stiffness E^{ref}_{50}	Unload-reload stiffness E^{ref}_{ur}, MPa	
1	SM	18.5	8	-		30	0	16	80	80
4.5	CL	18.4	2	54	0			8.1	41	41
10	CL	18.4	3	57				8.6	43	43
14.5	CL	18.4	4	60				9	45	45
17.5	CL	18.4	5	72				10.7	54	54
20.5	CL	19	6	88				13.2	66	66
25.5	CL	19	7	110				16.5	82	82
29.5	CL	19	9	130				19.5	97	97
33	CL	19.5	10	146	0			22	110	110
38.55	CL	19.5	20	173				26	130	130
46.5	SM	19.5	26	-	0	32	2	52	260	260
55.5	GM	21.9	>100	-	0	35	3	200	1000	1000

4.3 Determination of small-strain stiffness

The parameters for the small-strain stiffness, i.e., the G^{ref}_0 and the $\gamma_{0.7}$, for the Taipei clay have been determined from the laboratory tests. Chin et al. (2007) presents the K_0-consolidated undrained direct simple shear test (CK_0UDSS) results that depicted in Figure 7. Santos & Correia (2001) recommended that the stress-strain curve for small-strains can be described as:

$$G / G_0 = 1 / (1 + 0.385\ \gamma / \gamma_{0.7}) \quad (7)$$

where G_0 is the maximum small-strain shear modulus. The modulus degradation curves with the threshold $\gamma_{0.7}$ values ranging from 0.8×10^{-4} to 10^{-3} are shown in Figure 8. The degradation of the shear moduli with shear strain interpreted from the direct simple shear test is presented Figure 8, showing that the Taipei clay would have the $\gamma_{0.7}$ value of 5×10^{-4}. This $\gamma_{0.7}$ value is adopted for all the soil layers in this study. Since slurry trenching is mostly conducted in the clay layers, that $\gamma_{0.7}$ value of 5×10^{-4} for sand and gravel would not be influential to the analysis results.

Proceedings DOI: 10.21467/proceedings.171
ISBN: 978-81-970666-7-2

Series: AIJR Proceedings
ISSN: 2582-3922

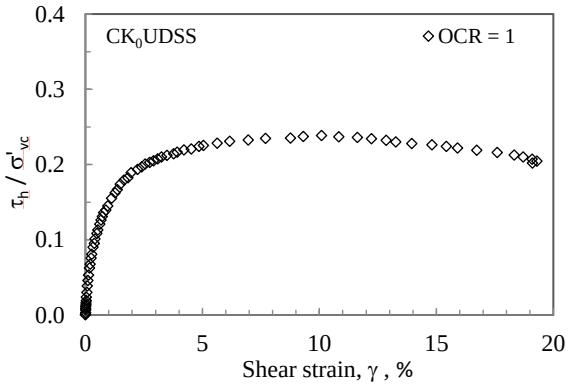

Figure 7: Stress-strain curve of Taipei clay under CK_0UDSS test (after Chin et al. 2007)

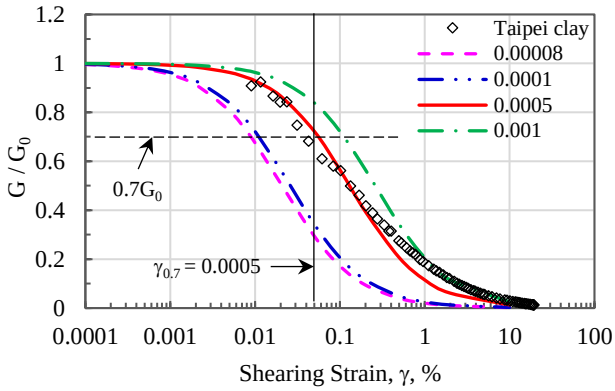

Figure 8: Degradation of shear moduli with shearing strain

4.4 Modeling of the slurry trenching

In the simulation for the trenching, the unit weight of 12 kN/m^3 for the slurry in the trench has been adopted. In reality, the slurry in the trench has no stiffness. However, as depicted in Figure 1, during excavating the primary wall panels, the trench is supported by the soil yet to be dug for installing the secondary panels, the concrete wall and the gravel infill. In the 2-D analysis, it is considered that the stiffnesses of materials supporting the trench, the quasi E_{trench} values, could be the weighted average of the Young's moduli of the slurry and the ground to be dug at the secondary wall panels.

In this study, the materials supporting the trench (ie., the slurry, in a sense) have been taken as the linear elastic materials. Based on the results of test runs, the E_{trench} values have been related to the E^{ref}_{50} values of the adjacent soil strata and the E_{trench} / E^{ref}_{50} ratios would vary from 0.001 to 0.2. The variation of the E_{trench} / E^{ref}_{50} ratios along the depth of the slurry trench are presented in Figure 9. The depths of the soil strata, h, are normalized with the depth of the slurry trench, the H value. It should be noted that this distribution of the E_{trench} / E^{ref}_{50} ratios is obtained from the results of back-analysis from the case history reporting in Section 5.1.

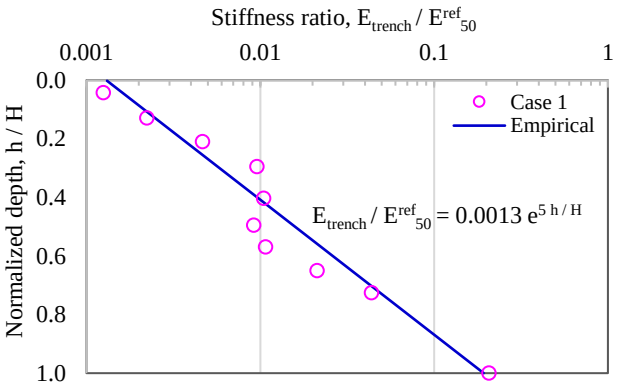

Figure 9: Variation of the stiffness ratios between the slurry trench and the adjacent soil

4.5 Cases analyzed

Three cases with different scenarios have been studied. For Case 1 there is no surcharge load. In Case 2, the surcharge pressure of 10 kPa is adopted to simulate the pressures imposed by the crawler cranes operating the clamshell buckets, lifting the reinforcement cages and for tremie concreting. The lateral extent of the surcharge area of 8 m is adopted. As mentioned in Section 3.4, the piezometric level of El. -5 m, which is the observed piezometric level in Jingmei Formation in 1993, has been adopted in Case 1 and Case 2.

The effect of ground water pressures to the ground movements due to diaphragm wall installation is studied in Case 3. The piezometric level in Jingmei Formation recovering to El. 5 m is adopted in the analysis. The

various conditions adopted for Case 1 to Case 3 are summarized in Table 2. For all the 3 cases the unit weight of the bentonite slurry of 12 kN/m^3 is adopted.

During excavation, the bentonite slurry in the trench is supposed to be maintained to the ground level. However, the clamshell bucket itself displaces part of the slurry in the trench. The top level of the slurry in the trench would drop when the bucket is lifted above the ground level to dispose the spoil. In the analysis, the top level of the slurry 2 m below the ground level is adopted to simulate this slurry displacing condition.

Guide walls were erected on both sides of the trench to prevent the ground from collapsing during slurry trenching. Due to the relatively shallow depth of the guide walls, the effect of installation of guide walls to ground movements is not simulated in this study.

Table 2: Cases studied for diaphragm wall installation

Scenario	Unit weight of slurry, kN/m^3	Piezometric level in Jingmei, El. m	Surcharge q, kPa	Main feature
Case 1	12	-5	0	No surcharge. Benchmark case.
Case 2		-5	10	Surcharge effect.
Case 3		5	0	Recovery in piezometric level with no surcharge.

5 RESULTS OF NUMERICAL ANALYSIS

5.1 Horizontal ground movements

The computed horizontal ground movements, the δ_h values, for Case 1 and Case 2 are presented in Figures 10 and 11. The computed maximum δ_h value at 2 m behind the wall for Case 1 is 26.4 mm. The analysis results are comparable with those observed at inclinometer SIS2, which was located next to a 12-storey building founding on bored piles. The pile toe levels are the same as that for the diaphragm wall. There would be no surcharge load imposing from the building foundation. Figure 10 shows that the computed maximum δ_h value of 26.4 mm is close to the observed value of 23.9 mm with the difference of 2.5 mm.

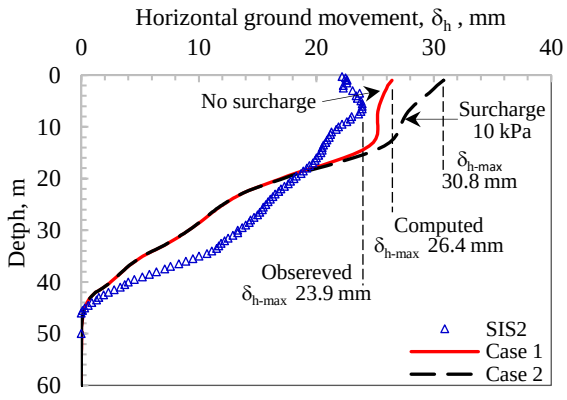

Figure 10: Computed horizontal ground movements at 2 m behind the wall compared with SIS2

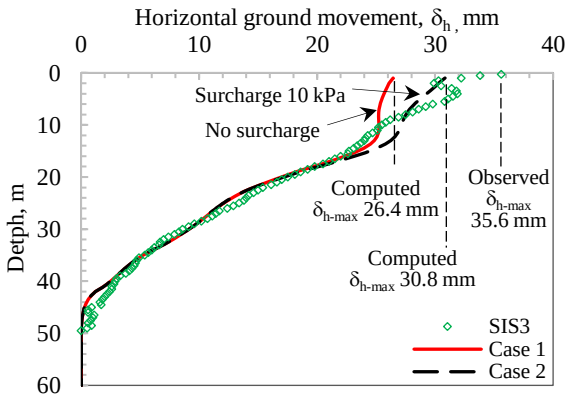

Figure 11: Computed horizontal ground movements at 2 m behind the wall compared with SIS3

5.2 Effect of surcharge

The computed δ_h values for Case 2 are compared in Figure 11 with those observed in inclinometer SIS3, which is located in the works area on the south side of City Hall Station. The crawler cranes operating could impose the surcharge load at the ground level and would affect the ground movements in the vicinity of SIS3. Figure 11 shows that the computed maximum δ_h value with surcharge is 30.8 mm, which is 4.4 mm larger than that of 26.4 mm without surcharge. The computed maximum δ_h value with surcharge of 30.8 mm is close to the 35.6 mm observed at SIS3, with the difference of 4.8 mm.

Proceedings DOI: 10.21467/proceedings.171
ISBN: 978-81-970666-7-2

Series: AIJR Proceedings
ISSN: 2582-3922

5.3 Effect of groundwater pressures

The groundwater pressure would have critical effect to ground movements. The computed δ_h values for Case 3 are presented in Figure 12. The numerical analysis shows that with the piezometric levels recovering from El. -5 m to El. +5 m, the maximum δ_h value could increase by 11.3 mm, from 26.4 mm to 37.7 mm.

As described in Section 3.4, the piezometric level in the Jingmei Formation was drawn-down to near the bottom level of the Songshan Formation in the 1970s. The lateral pressure increment acting on the slurry trench would be low and stable trench excavation have been experienced. With the piezometric levels in the Jingmei Formation fully recovering to close to the ground surface in recent years, say in 2024, the horizontal pressures acting on the trench would be larger than those previously experienced. The past stable and minimal ground movements induced by wall trenching would no longer be taken for granted.

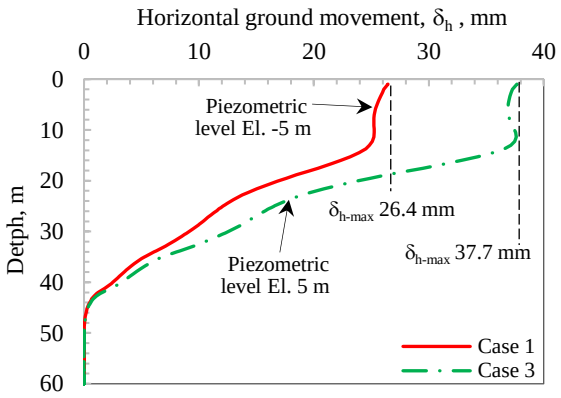

Figure 12: Computed horizontal ground movements with the piezometric level recovered to El. 5 m

5.4 Vertical ground movements

The computed vertical ground movements, the δ_v values, for Case 1 and Case 2 are presented in Figure 13. For Case 1 with no surcharge, the computed maximum δ_v values immediately behind the wall would be 20.8 mm. The maximum δ_v value for Case 2 with 10 kPa surcharge would be 26.9 mm, which is 6.1 mm larger than that without surcharge. As there is no settlements data in the diaphragm wall installation stage for City Hall Station (BL18), the settlements observed at the adjacent metro stations are collected for comparison.

Ou & Yang (2011) reported the settlements observed at Zhongxiao-Fuxing Station (BL16) and at Yongchun Station (BL19). The settlements were observed upon completion of the entire perimeter diaphragm walls of these stations. Station BL16 is located at 2 km west of Station BL18. Station BL19 is located at 1 km east of Station BL18. The diaphragm wall at Station BL16 was 1.0 m in thickness and 41 m in depth. The combined thickness for the clayey sublayers IV and II was 26 m. According to Chen et al. (1997), the diaphragm wall at Station BL19 was 1.2 m in thickness and 38 m in depth and the total thickness for the sublayers IV and II was 34 m. The wall lengths and the soil conditions at Stations BL16 and BL19 are similar to those at Station BL18.

Figure 13 presents the surface settlements, the δ_v values, observed at Station BL16. At the distance around 10 m behind the wall, the observed δ_v values range from 4.4 mm to 36.7 mm, with the mid value of 20.5 mm. At that distance, the computed settlement profile for Case 1 with no surcharge has the δ_v value around 18 mm, which is close to the average settlement observed.

The surcharge adopted in the analysis extends from 2 m to 10 m behind the wall. The 10 kPa surcharge would cause the computed maximum δ_v value of 26.9 mm. Figure 13 shows that the upper bound envelope of the observed settlements would be caused by the surcharge load. Such surcharge would likely be attributable to the operation of the crawler cranes for installation of the wall panels.

Figure 13 shows wide scattering of the settlements observed. One of the probable reasons for the lower bound envelope is that some of the settlement points were installed on pavements. Some of the settlement points were underlain by utilities such as the water mains, stormwater drains, sewer pipes and gas pipes. In future studies, settlements data affected by utilities shall be sorted out for fair comparison. It is very likely that the upper bound envelope of the measurement would be closer to free-field ground response. On the other hand, some settlements

would be induced by consolidation, which is not considered in the analyses. Besides, the possibility that some of the settlement points were disturbed by traffic cannot be ruled out.

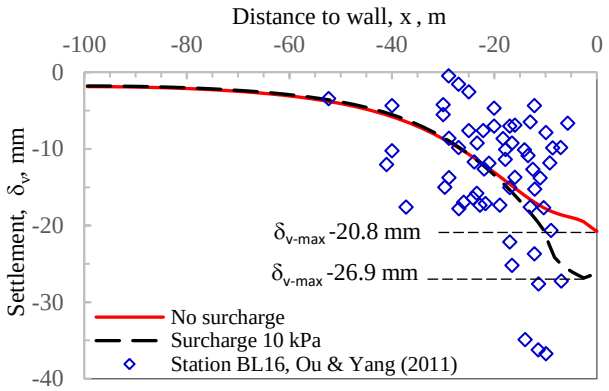

Figure 13: Computed settlements behind the wall with and without surcharge

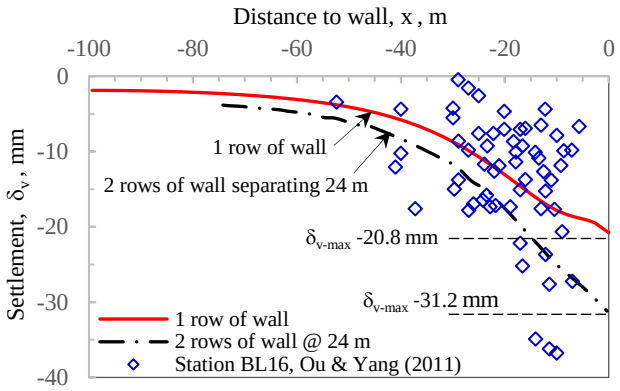

Figure 14: Computed settlements behind the wall induced by 2 rows of slurry trench

5.5 Multi-row of wall installation

Figure 13 shows that the settlements induced by slurry trenching would have wide lateral extent. At the distance of 24 m behind the wall, the computed δ_v value would be around 10 mm, which is about 50 % of the maximum δ_v value of 20.8 mm immediately behind the wall for the case with no surcharge.

As shown in Figure 2, City Hall Station was retained by 2 rows of diaphragm wall separating apart by 24 m. Installation for these 2 rows of wall could have the superimposing effect to the ground movements. The computed result for Case 1 gives the settlements caused by installing the single row of wall located at the near side. Shifting the computed profile to the other side by 24 m gives the settlements caused by installation of the wall located on the far side.

The combined settlements profile for the 2 rows of slurry trenching are presented in Figure 14. The computed maximum δ_v value immediately behind the wall caused by installing the single row would be 20.8 mm. That δ_v value would increase to 31.2 mm by adding the settlements induced by the earlier installation of the wall on the far side, with an increment of 10.4 mm. As the computed settlements profile for installing 2 rows of slurry trench fall into the upper bound envelope of those observed at Station BL16, the superimposing effect is verified by the field observation.

5.6 Normalized settlement profiles

Figure 15 presents the settlements observed at Station BL19. The observed settlements, δ_v, and the distances to the wall, x, are normalized with the depth of the slurry trench, H. The H value for the slurry trench of City Hall Station is 44.5 m.

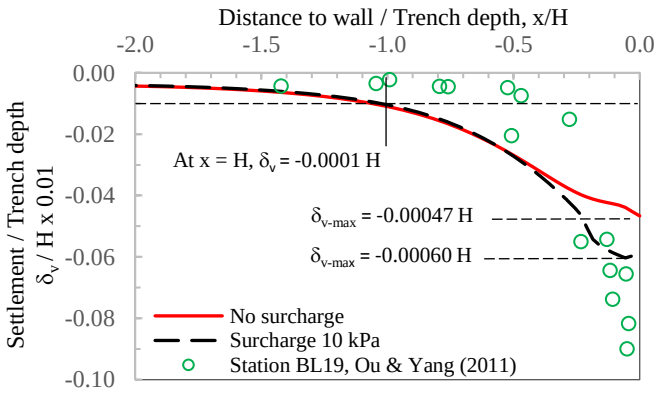

Figure 15: Normalized observed and computed settlements behind the wall

Proceedings DOI: 10.21467/proceedings.171
ISBN: 978-81-970666-7-2

Series: AIJR Proceedings
ISSN: 2582-3922

Figure 15 also shows the similar trend that the observed upper bound settlements envelope would be attributable to the surcharge load. Both Figures 13 and 15 show the agreement between the computed and the observed settlements caused by diaphragm wall installation. Figure 15 shows that the settlement trough induced by slurry trenching would have the extent of 1H. At that distance, the δ_v value would be around 20 % of the maximum δ_v value occurring immediately behind the wall for the case with no surcharge. The maximum δ_v value immediately behind the wall would be 0.00047H and 0.0006H for the cases without and with surcharge respectively.

6 CONCLUSIONS

A 2-Dimensional numerical analysis have been conducted for assessing the ground movements caused by diaphragm wall installation. The nonlinear Hardening-soil with Small-strain stiffness (HSS) soil model is adopted for the soil materials. The following conclusions could be drawn:

(1) In the case histories reported in this study, both the observed horizontal and vertical ground movements caused by diaphragm wall installation were as large as 36 mm. Such large magnitude of ground movements should not be over-looked from the buildings protection point of view.
(2) In addition to the unit weight of the bentonite slurry that would affect the performance of the ground movements, the surcharge due to the construction plants for wall installation would have significant effect to ground movements.
(3) The superimposing effect of ground movements due to installation multi-rows of slurry trenches shall be considered, especially where the horizontal distance between 2 rows of slurry trench would be less than 1 time the depth of the trench and at the entrances.
(4) Taking 20 % maximum settlement occurring immediately behind the wall as the criterion, the settlement trough induced by slurry trenching would have the influence of 1 time the depth of the trench.
(5) The groundwater pressure would have critical effects to ground movements. The numerical analysis in this study shows that with the piezometric levels recovering from El. -5 m to El. +5 m, the maximum horizontal ground movements could increase from 26.4 mm to 37.7 mm. With the piezometric levels fully recovering in recent years, the stable and minimal ground movements induced by wall trenching experienced in the past decades would no longer be taken for granted.

The building foundations would affect the magnitude of ground movements. In the next studies, the ground movements due to the surcharge imposing from the nearby shallow foundations shall be considered.

There is an empirical approach that the slurry trench would have some virtual stiffness, which is the weighted average of the stiffness of the surrounding soil along the trench. The empirical stiffness values for the trench have been calibrated against the observed horizontal ground movements. The application of the empirical relationship between the trench stiffness and the soil stiffness to other geological zones shall be verified with more observed case histories.

This study provides the method of replacing the soil unit weights with that of the bentonite slurry in the numerical analysis on the ground movements induced by wall installation. The method would be a simplified approach as an alternative to the more sophisticated 3-Dimensional analysis. With the proposed 2-Dimensional approach, the stress histories due to trenching could be properly assessed. The wish-in-place for wall could no longer be assumed in the analysis on the following construction such as station excavation and jet grouting.

ACKNOWLEDGEMENTS

The Author wishes to express his sincerely thanks to Dr R.N. Hwang of Moh and Associates, Inc. for providing the field observation data on diaphragm wall construction and his valuable advices on this study.

PUBLISHER'S NOTE

AIJR remains neutral with regard to jurisdictional claims in published maps & institutional affiliations.

HOW TO CITE

L.W. Wong (2024). Ground Movements Caused by Diaphragm Wall Installation. *AIJR Proceedings*, 272-283. https://doi.org/10.21467/proceedings.171.24

REFERENCES

Benz, T. (2006). Small-strain stiffness of soils and its numerical consequence. *Dissertation of thesis*, the Institute of Geotechnics, University Stuttgart.

Chen, Y. K., Huang, C. C. & Wang, F. G. (1997). Grouted raft for building protection in excavation in soft clay. *Proceedings of 7th Conference on Current Research in Geotechnical Engineering*, Chinshan, Taiwan, August 1997, Vol. 1: 593-600. (in Chinese)

Chin, C.T., Chen, J.R., Hu, I.C., Yao, D.H.C. & Chao, H.C. (2007), Engineering characteristics of Taipei clay. In T.S. Tan, K.K. Phoon, D.W. Hight & S. Leroueil (Eds), entitled*: Characterization and Engineering Properties of Natural Soils,* Taylor & Francis Group, v3: 1755-1803.

Chin, C.T., Crooks, A.J.H. & Moh, Z.C. (1994). Geotechnical properties of the cohesive Sungshan deposits. *Geotechnical Engineering, J. Southeast Asian Geotechnical Society*, Taipei, Taiwan 25(2): 77-103. (in Chinese)

Chin, C.T. & Liu, C-C. (1997). Volumetric and undrained behaviors of Taipei silty clay. *J. Chinese Institute of Civil and Hydraulic Engineering*, Taipei, Taiwan 9(4): 665-678. (in Chinese)

Cowland, J.W. & Thorley, C.B.B. (1985). Ground and building settlement associated with adjacent slurry trench excavation, *Ground Movements and Structures*, Pentech Press, London, UK: 723-738.

Hwang, R. & Moh, Z.C. (2022). Groundwater drawdown and subsidence in the Taipei Basin. *Sino-Geotechnics,* No. 173/2022.9: 99-110. (in Chinese)

Hu. I.C., Chin, C.T. & Liu, C.J. (1996). Review of the geotechnical characteristics of the soil deposits in Taipei, *Sino-Geotechnics*, No. 54: 5-14. (in Chinese)

Kung, G.T.C, Ou, C.Y. & Juang C.H. (2009). Modelling small-strain behavior of Taipei clays for finite element analysis of braced excavations. *Computers and Geotechnics* 36 (2009): 304-319.

MAA (1987) *Engineering properties of the soil deposits in the Taipei Basin*, Report No. 85043, Ret-Ser Engineering Agency and Taipei Public Works Department, Taipei. (in Chinese)

Moh, Z.C. & Ou C.D. (1979). Engineering characteristics of Taipei Silt. *Proc., 6th Asian Regional Conference on Soil Mechanics and Foundation Engineering*, Singapore, 1: 155-158.

Moh, Z.C., Chin, C.T., Liu, C.J. & Woo, S.M. (1989). Engineering correlation for soil deposits in Taipei. *J. Chinese Institution of Engineers*, 124(9): 798-808.

Morton, K., Cater, R.W. & Linney, N. (1980). Observed settlements of buildings adjacent to stations constructed for the modified initial system of the mass transit system, Hong Kong. *Proceedings of the 6th Asian Conference of the Soil Mechanics and Foundation Engineering*, Taipei, Vol. 1: 415-429.

Ng, C.W.W., Lings, M.L., Simpson, B. & Nash, D.F.T. (1995). An approximate analysis of the three-dimensional effects of diaphragm wall installation. *Geotechnique* 45, No.3: 497-507.

Ou, C.Y. & Yang, L.L. (2011). Observed performance of diaphragm wall construction. *Geotechnical Engineering Journal of the SEAGC & AGSSEA*, Vol. 42, No.3, September 2011. ISSN 0046-5828: 41-49.

Ou, C.Y., Liao, J.T. & Cheng, W.L. (2000), Building response and ground movements induced by a deep excavation, *Geotechnique*, Vol. 50, No. 3: 209-220.

PLAXIS B.V. (2013). *PLAXIS Reference Manual*. PLAXIS, BV, Delft, the Netherlands.

Santos J.A. & Correia, A.G. (2001). Reference threshold shear strain of soil. Its application to obtain a unique strain-dependent shear modulus curve for soil. *In 15th Int. Conf. SMGE*, Volume 1, Istanbul, A.A. Balkema. 267-270.

Schanz, T. & Vermeer, P.A. (1998). On the Stiffness of Sands. *Geotechnique,* 46, No. 1: 145-151.

Schanz, T., Vermeer, P.A. & Bonnier, P.G. (1999). The hardening soil model: formulation and verification. *Beyond 2000 in Computational Geotechnics*. Rotterdam, the Netherlands: 281-290.

Wong, L.W. (2023). Effects of soil-structure interaction on wall deflections and surface settlements during deep excavations. *Proceedings, 43rd HKIE Geotechnical Division Annual Seminar*, Hong Kong, May: 70-81.

Proceedings DOI: 10.21467/proceedings.171
ISBN: 978-81-970666-7-2

Series: AIJR Proceedings
ISSN: 2582-3922